NeuroImage: Clinical 28 (2020) 102410

Contents lists available at ScienceDirect

NeuroImage: Clinical

journal homepage: www.elsevier.com/locate/ynicl

Structure-function abnormalities in cortical sensory projections in embouchure dystonia

Tobias Mantel[a], Eckart Altenmüller[b], Yong Li[a], André Lee[a,b], Tobias Meindl[a], Angela Jochim[a], Claus Zimmer[c], Bernhard Haslinger[a,*]

[a] Department of Neurology, Klinikum rechts der Isar, Technische Universität München, Ismaningerstrasse 22, Munich, Germany
[b] Hochschule für Musik, Theater und Medien Hannover, Emmichplatz 1, Hanover, Germany
[c] Department of Neuroradiology, Klinikum rechts der Isar, Technische Universität München, Ismaningerstrasse 22, Munich, Germany

ARTICLE INFO

Keywords:
Musician's Dystonia
Dystonia, Focal, Task-Specific
Diffusion Tractography
Sensorimotor Cortex
Basal Ganglia

ABSTRACT

Background: Embouchure dystonia (ED) is a task-specific focal dystonia in professional brass players leading to abnormal orofacial muscle posturing/spasms during performance. Previous studies have outlined abnormal cortical sensorimotor function during sensory/motor tasks and in the resting state as well as abnormal cortical sensorimotor structure. Yet, potentially underlying white-matter tract abnormalities in this network disease are unknown.
Objective: To delineate structure-function abnormalities within cerebral sensorimotor trajectories in ED.
Method: Probabilistic tractography and seed-based functional connectivity analysis were performed in 16/16 ED patients/healthy brass players within a simple literature-informed network model of cortical sensorimotor processing encompassing supplementary motor, superior parietal, primary somatosensory and motor cortex as well as the putamen. Post-hoc grey matter volumetry was performed within cortices of abnormal trajectories.
Results: ED patients showed average axial diffusivity reduction within projections between the primary somatosensory cortex and putamen, with converse increases within projections between supplementary motor and superior parietal cortex in both hemispheres. Increase in the mode of anisotropy in patients was accompanying the latter left-hemispheric projection, as well as in the supplementary motor area's projection to the left primary motor cortex. Patient's left primary somatosensory functional connectivity with the putamen was abnormally reduced and significantly associated with the axial diffusivity reduction. Left primary somatosensory grey matter volume was increased in patients.
Conclusion: Correlates of abnormal tract integrity within primary somatosensory cortico-subcortical projections and higher-order sensorimotor projections support the key role of dysfunctional sensory information propagation in ED pathophysiology. Differential directionality of cortico-cortical and cortico-subcortical abnormalities hints at non-uniform sensory system changes.

1. Introduction

Embouchure dystonia (ED) is a task-specific focal dystonia (TSFD) manifesting in highly-trained brass players during musical performance. In the otherwise asymptomatic patients, playing the instrument evokes abnormal posturing, tremor, and spasms in the (peri)oral muscles that control the airflow through the mouthpiece, severely disabling musical performance (Frucht, 2009). Abnormal sensorimotor information integration has been postulated a central feature with regard to the manifestation of dystonic postures. Observations during both task and rest in ED suggest that this dysfunctional integration may encompass primary and higher-order sensorimotor cortices (Haslinger et al., 2010, 2017). Maladaptive plasticity, abnormal intracortical/basal ganglia inhibition, and abnormal processing of sensory information are assumed the most relevant pathophysiologic mechanisms leading to sensorimotor dysfunction in the disease (Quartarone and Hallett, 2013). Yet, the exact nature of their interplay eventually resulting in the cortical frontoparietal (e.g. sensorimotor) network abnormalities observable using functional

Abbreviations: AD, axial diffusivity; ADDS, arm dystonia disability scale; CON, healthy musicians; dMRI, diffusion MRI; DTI, diffusion tensor image; ED, embouchure dystonia, FA, fractional anisotropy; FD, focal dystonia; FDR, false discovery rate; FWE, family-wise error; GM, grey matter; M1, primary motor cortex; MO, mode of anisotropy; PAT, brass players with embouchure dystonia; Put, Putamen; RD, radial diffusivity; ROI, region of interest; rsfMRI, resting state functional MRI; S1, primary somatosensory cortex; SLF, superior longitudinal fascicle; SMA, supplementary motor area; SPL, superior parietal lobe; TE/TR, echo/repetition time; TSFD, task-specific focal dystonia

* Corresponding author.
E-mail address: bernhard.haslinger@tum.de (B. Haslinger).

https://doi.org/10.1016/j.nicl.2020.102410
Received 7 May 2020; Received in revised form 29 July 2020; Accepted 30 August 2020
Available online 02 September 2020

neuroimaging is unclear (Haslinger et al., 2017). Previous findings in musician's dystonia favour an emphasized role of abnormal (somato) sensory processing in orderly predisposed individuals in the emergence of this form of TSFD (Lim et al., 2003; Rosenkranz et al., 2005). Sensory dysfunction in ED has been observed both in presence and in absence of tasks (Haslinger et al., 2010, 2017; Mantel et al., 2016), accompanied by reports of abnormal somatosensory topography and grey matter (GM) volume hinting at maladaptive plasticity in such cortices (Mantel et al., 2019, 2016; Uehara et al., 2019). Subcortically, findings in ED during task paradigms and in structural analysis both in embouchure and pianist's musician's dystonia point to particular relevance of the striatum (Granert et al., 2011; Haslinger et al., 2010; Mantel et al., 2019). This is in line with recent observations in non-musician TSFD suggesting an abnormal dopamine receptor expression in both motor and nonmotor sections of the striatum, which may in turn result in a reduced inhibition/increased excitation in the cortex due to an imbalance in basal-ganglia outflow pathways (Fujita and Eidelberg, 2017; Simonyan et al., 2017).

Based on the evidence outlined above, this work aimed at further structuro-functional characterization of abnormal cerebral sensorimotor interaction patterns in ED focusing on projections of cortical origin. Following the previously reported abnormalities in ED, a simple model mirroring basic cerebral sensorimotor interaction involving primary and higher-order sensory and motor cortices and the putamen (due to its role as main entry point of cortical input to the basal ganglia) was set up. This allowed to sensitively investigate the integrity of structural and functional sensory and motor trajectories with regard to their inter- and subcortical relations, focusing on trajectories within which we hypothesized abnormalities in tract integrity (and concomitant functional changes) to be most likely to occur based on the existing evidence.

2. Methods

2.1. Participants

The study included 16 professional brass musicians with ED (44.2 ± 12.4 years, 14 males, 2 females; PAT) recruited from the Institute for Music Physiology and Musicians Medicine in Hanover, and 16 healthy professional brass players recruited from local conservatories/orchestras (44.1 ± 12.1 years, 16 males; CON). All were right-handed (Oldfield, 1971) musical professionals with no (other) neuro(psychiatric) deficits or symptoms (including no other movement disorders), no major internal disease and no abnormal brain structure on MRI (table 1 for details). No patient was treated with botulinum neurotoxin (15 patients were never treated; one patient had received one injection 20 months prior to participation) or under the effect of oral medication for dystonia at the time of the study. The study was approved by the institutional ethics board (Ethikkommission der Technischen Universität München, https://www.ek-med-muenchen.de). All participants gave written informed consent according to the Declaration of Helsinki. In addition to MRI acquisition, each participant's lower face and neck were videotaped during musical performance of predefined sequences (ascending/descending scales, fourths, tones). Given insensitivity of established focal dystonia (FD) rating scales (e.g. Burke-Fahn-Marsden, Tubiana-Chamagne score) to ED-specific symptoms such as deterioration of sound or attack of the tongue, video performances were blindly rated by an ED expert (E.A.) according to a previously employed customized score (Haslinger et al., 2010, 2017; Mantel et al., 2019, 2016). Further, the Arm Dystonia Disability Scale (ADDS) was collected to screen for possible co-incident symptoms of hand TSFD.

2.2. Data acquisition

Data were acquired on a 3T Achieva MRI scanner (Philips, the Netherlands) with an 8-channel head coil. First, 64-gradient direction diffusion tensor MR images (dMRI) were acquired using a cardiac-gated single-shot spin-echo echo-planar imaging sequence (echo time (TE) = 92 ms, repetition time (TR) = 11–22 bpm (heart-rate dependent), b-value = 1400 s/mm^2, α = 90°; field-of-view = 232 × 232 mm; voxel size = 1.81 × 1.81 × 2 mm^3; 66 axial slices without gap). Participants' heads were fixed with foam pads to minimize the risk of motion artefacts. To further reduce motion risk in view of relatively long dMRI scan durations owed to cardiac gating, image acquisition was divided into two separate runs of 32 diffusion-weighted images each. Second, 303 echo-planar resting-state functional MR images (rsfMRIs) were collected (TR/TE = 2200/30 ms, field-of-view = 216 × 216 mm^2, voxel size 3 × 3 × 3 mm^3, 36 axial slices, gap 0.5 mm). Participants were instructed to keep their eyes closed during the whole measurement. Third, a 3D high-resolution gradient echo T1-weighted reference image was acquired (TR/TE/inversion time = 9/4/780 ms; α = 8°; field-of-view = 240 × 240 mm, voxel size 1 × 1 × 1 mm^3, 170 axial slices without gap).

2.3. Software

dMRI data were preprocessed using ExploreDTIv4.8.6 (www.exploredti.com) and analysed in FSLv5.0.10 (https://fsl.fmrib.ox.ac.uk/fsl/). RsfMRI data were analysed in SPM12br6906 (https://www.fil.ion.ucl.ac.uk/spm/) and DPABIv3.0. Anatomical scans were processed in CAT12r1152 (http://www.neuro.uni-jena.de/cat/). Statistical analysis was performed using PALMα112 (https://fsl.fmrib.ox.ac.uk/fsl/fslwiki/PALM), MatlabR2016b (the MathWorks Inc., Natick, USA), and SPSS25 (IBM, New York, USA).

2.4. Diffusion data analysis

2.4.1. Preprocessing

dMRI data from the two runs were concatenated, corrected for motion/eddy current-induced geometrical distortions (Leemans and Jones, 2009) and for susceptibility-induced distortion aided by information from the aligned anatomical scan (Irfanoglu et al., 2012) with upsampling to a voxel size of 1 mm isotropic. Registration and data quality were visually checked. *BEDPOSTx* was applied to fit a probabilistic diffusion model on the corrected data, modelling two fibres per voxel. Scalar images were calculated from the diffusion tensor images (DTI) based on a linear tensor model using *DTIFIT*.

2.4.2. Probabilistic tractography

Following the study's objective, we set up a simple model mirroring potentially abnormal intracerebral trajectories of sensorimotor integration originating from the cortical level: probabilistic tractography was performed to reconstruct connections between (i) the superior parietal lobe (SPL) and supplementary motor area (SMA) within the superior longitudinal fascicle (SLF) (Bozkurt et al., 2017; Makris et al., 2005), (ii) the facial primary somatosensory ($S1_{FACE}$) and facial primary motor cortex ($M1_{FACE}$), (iii) the SMA and $M1_{FACE,}$ and (iv) these cortical areas and the putamen (Put). All regions fulfilled our internal reliability requirement of having been reported abnormal in musician's or embouchure dystonia in more than one study and more than one neuroimaging approach (Granert et al., 2011; Haslinger et al., 2010, 2017; Kita et al., 2018; Mantel et al., 2019, 2016). The cortical regions of interest (ROIs) were derived from the Brainnetome atlas (https://atlas.brainnetome.org/) (Fan et al., 2016), whose detailed connectivity-based cortical parcellation makes it advantageous for analyses using corresponding modality. The subcortical putamen ROIs (serving as target only, see below) were derived from the Harvard-Oxford subcortical atlas (https://fsl.fmrib.ox.ac.uk/fsl/), achieving good overlay with the subject basal ganglia macroanatomy with reliable exclusion of neighbouring white matter of the capsule (table s-1A). Tract reconstruction was performed in native space pursuing a previously described two-pass procedure that allows for reliable reconstruction of trajectories with small structural connectivity probabilities (Schulz et al., 2015). Tracking was performed from the juxtacortical white

Table 1
Demographic and clinical characteristics.

	brass musicians with ED		healthy brass musicians	p-value
Age, y (mean, SD)	44.2, 12.4		44.1, 12.1	0.98[1)]
Sex (m/f)	14/2		16/0	0.10[2)]
TIV, cm^3 (mean, SD)	1604.8		1593.5	0.79[1)]
age at start of play, y (mean, SD)	11.2, 2.5		11.0, 3.8	0.82[1)]
main instrument (trumpet/trombone/horn)	4/8/4		3/3/10	
Disease duration, mo	65.8, 50.7			
Daily training, h (median, IQR)[a]	before ED	4.0, 1.8	2.5, 1.3	0.005[2)] / 0.002[3)](between/within-group)
	with ED	0.9, 2.0		
ED score (median, IQR)[b]	4.0, 1.8		1.0, 0	< 0.001[2)]
ADDS (mean, SD)	99.4, 1.7			

Demographic and clinical characteristics of healthy and diseased brass musicians. To further account for potential nuisance effects of age, sex and total intracranial volume (TIV), these variables were additionally included as nuisance covariates in statistical analyses where appropriate (see section 'Statistical analyses'). Statistical between-group comparisons applied [1)]t-tests, [2)]Wilcoxon rank-sum or [3)]signed-ranks tests. Evaluation by both ADDS and neurologic exam did not reveal signs of signs of concomitant hand dystonia in patients. SD = standard deviation; IQR = interquartile range; y = years; h = hours; TIV = total intracranial volume; m = male; f = female; NA = not applicable.

[a]Based on retrospective reports. For daily training at the time of the study, the average for the last four weeks was indicated. Given the nature of the disease, daily training was reduced after disease onset compared to healthy brass players.

[b]Embouchure dystonia score (dystonic symptom rating during performance of standardized sequences): 1 = normal play, 2 = nearly normal play, not distinctly dystonic; 3–5 = abnormal playing with evidence of dystonic orofacial movements (minor/medium/severe degree).

matter: following atlas registration to the individuals' native space applying the warping parameters generated during segmentation and Montreal Neurological Imaging (MNI) space normalisation of the aligned anatomical scan, the final native-space tractography seeds for each participant were generated by multiplication of the atlas-derived ROIs with a Ø 2 mm white matter surface margin generated by respective erosion of the aligned anatomical native space white matter segment (figure s-1). For cortico-cortical connections 50,000 streamlines were sent reciprocally from the seeds and combined (Jeurissen et al., 2019; Schulz et al., 2015), and for cortico-putaminal connections 25,000 streamlines were sent unidirectionally form the cortical seeds (curvature threshold 0.2, step length 0.5 mm) in native space. Tracking was constrained to voxels with FA > 0.15 which reliably prevented tracking through non-white matter tissue. For initial tract reconstruction, anatomy-informed standardized exclusion masks created on literature-based knowledge on tract courses (Kamali et al., 2014; Lehericy et al., 2004) were applied to guide tractography (table s-1B). Notably, these encompassed subcortical nuclei of no interest, passages to the brainstem/through the internal capsule, GM, cerebrospinal fluid, and neighbouring juxtacortical white matter to exclude erroneous tract propagation through U-fibres. In a second step, refined exclusion masks were generated by mean dilation of the initial trajectory volume four times at a common 5% threshold and further addition of specific exclusion masks (if necessary) to eliminate erroneous fibre courses. After refinement in this second pass, resulting individual tracts were thresholded at connection probabilities of 2%, 5%, 10%, and 20%. Mean values of fractional anisotropy (FA), the (orthogonal) mode-of-anisotropy (MO), axial (AD) and radial diffusivity (RD) were extracted from the individual tract volumes in native space for evaluation of tract integrity. As there is no objective standard for thresholding in probabilistic tractography we chose not to investigate a single threshold but calculated the mean across the above thresholds (Schulz et al., 2015). Given that cortico-(sub)cortical $M1/S1_{FACE}$-seeded probable tracts run in close proximity, we calculated Jaccard's coefficients (range 0–1; 0 = full dissimilarity, 1 = full similarity) for each participant to detect relevant overlays.

2.5. Functional data analysis

2.5.1. Preprocessing

Data preparation included discarding of the first five scans, realignment, slice-timing correction (to first slice), coregistration with the anatomical scan, and normalization to MNI space applying anatomical scan-derived warping parameters. This was followed by linear detrending, regression of six motion parameters, scrubbing of scans with framewise displacement > 0.5 mm (including the preceding and two following scans) (Jenkinson et al., 2002), removal of five white matter and cerebrospinal fluid signal principal components (CompCor), and bandpass-filtering (0.01–0.08 Hz). Scans were smoothed with a 6 mm full-width-at-half-maximum Gaussian kernel.

2.5.2. Seed-based correlation analysis

ROI-based functional connectivity (FC) analysis was conducted for all eight cortical ROIs in MNI space. Following ROI intersection with the individual GM, seed-to-voxel correlations in each subject were calculated through Pearson correlation of voxel-averaged time courses within each ROI with all other voxels in the brain (figure s-1). Correlation coefficients were Fisher-z-transformed. Given the study objective, subsequent statistical analysis was constrained to voxels within the combined volume of each ROIs respective target areas investigated during tractography.

2.6. Post-hoc analysis of grey matter volume

We were further interested if abnormal trajectories might originate from areas of abnormal GM structure. Yet, the sample size in the present study was not suitable for a comprehensive evaluation of GM structure. We hence conducted a planned post-hoc volumetric analysis in cortices previously reported structurally abnormal in ED (Mantel et al., 2019), in case consistent structure–function abnormalities in trajectories involving this cortex were found. Volumetry of absolute GM volumes was performed applying the same cortical ROI as during the respective FC analysis to the subjects' DARTEL (Diffeomorphic Anatomical Registration Through Exponentiated Lie Algebra)-normalized, modulated, nonsmoothed GM.

2.7. Statistical analyses

Between-group differences in tract integrity measures, FC and GM volume were analysed applying two-tailed permutation testing according to the Freedman-Lane approach (Winkler et al., 2014, 2016), calculating 10,000 permutations for image and 100,000 permutations for non-image data. Voxel-wise FC analysis results were voxel-level family-wise error (FWE)-corrected. The significance level in all analyses was set at $\alpha = 0.05$, with estimated p-values in each analysis false discovery-rate (FDR)-adjusted for multiple comparisons (i.e. 14

investigated tracts, 8 FC analyses, and the number of GM volumes analysed *post-hoc*). All statistical analyses were adjusted for potential effects of age and sex; for analyses involving GM, the total intracranial volume was additionally included. Beyond exploration of structuro-functional associations in case of coincident differences in a trajectory, adjunct linear regression analyses with clinical parameters (disease duration, severity by ED score) within patients were added for significant between-group differences.

2.8. Control analyses

(i) In order to assess whether potential significant structural/functional abnormalities in the primary somatosensory or motor cortex were also present in clinically non-affected areas of those cortices, control analyses for tractography/functional connectivity/grey matter volumetry results were performed for a medial Brainnetome atlas parcel most likely comprising the trunk/neck area within the respective primary cortices, provided that the results in the main analysis was significant. (ii) To control for the possibility of local FC potentially affecting remote FC abnormalities (Jiang and Zuo, 2016) we additionally tested for abnormalities of regional homogeneity between groups. For this assessment, we calculated Kendall's coefficient of concordance on the normalized, nuisance signal-regressed, bandpass-filtered (0.01–0.08 Hz) functional data. Data were then Fisher-z-transformed, and smoothed with a 6 mm full-width-at-half-maximum Gaussian kernel. (iii) To assess whether potential structure–function associations were specific to ED, the respective regression analyses were repeated for the healthy control group in case of significant results.

3. Results

3.1. Probabilistic tractography of sensorimotor trajectories

Tractography yielded probable trajectories connecting the primary/higher-order sensorimotor cortices and the putamen in all subjects. Probable tracts connecting sensory and motor cortices were reconstructable in all subjects for primary $S1_{FACE}$ -$M1_{FACE}$ connections, and in > 90% of participants for the higher-order SPL-SMA connection. Trajectories connecting parietal and frontal lobes ran distinct courses either in the SLF1 (SPL-SMA) or the lateral portion of the SLF2/the U-fibres ($S1_{FACE}$-$M1_{FACE}$). The intercortical trajectory between SMA and $M1_{FACE}$ showed lesser reconstructability (left hemisphere 78%, right hemisphere 84% of participants). Beyond technical aspects given the abundance crossing fibres in the frontal central white matter, the reason for this difficulty remained unclear. Subcortical tract terminations followed the putaminal topography (Tziortzi et al., 2014) (Fig. 1). In comparable trajectories, spatial variability of tract courses mirrored by reduced spatial overlay of tract volumes with increasing probability thresholds was higher in trajectories of sensory than of motor cortical origin, and rather elevated in trajectories involving higher-order compared to primary cortices, probably attributable to the higher cortical variability in such areas (figure s-2 for details of the descriptive evaluation) (Schulz et al., 2015). Reconstruction of cortico-subcortical and cortico-cortical tracts involving the primary sensorimotor cortices was possible without relevant overlay between the different tracts across analysed thresholds (table s-2).

3.2. Analyses of tract-related white matter integrity

Between-group analysis revealed significantly reduced AD in the left- and right-hemispheric trajectories between $S1_{FACE}$ and the putamen in ED patients compared to healthy brass players. Conversely, AD was significantly increased in ED patients compared to healthy brass players in the projections between SPL and SMA in both hemispheres. In the left hemisphere, this was accompanied by a significant increase in MO in ED patients compared to healthy brass players. Furthermore, ED patients showed significantly increased MO in the left-hemispheric trajectory connecting $M1_{FACE}$ and SMA compared to controls (table 2 for details, table s-3 for other DTI scalars and trends).

3.3. Analyses of related functional connectivity profiles

FC analysis revealed significantly reduced connectivity of the left $S1_{FACE}$ with the sensorimotor area in the left putamen ($x|y|z = -24|-8|7$; $p_{FWE} = 0.015$, FDR-adjusted) in ED patients compared to controls, the cluster being located inferior to the termination of the white matter tract between $S1_{FACE}$ and the putamen (Fig. 2A). Other analyses did not yield significant results.

3.4. Post-hoc structural analyses

Based on the above results, between-group volumetric GM analysis was performed for the left putamen and $S1_{FACE}$. This revealed increased GM volume in ED patients in left $S1_{FACE}$ ($p_{FDR} = 0.039$; Fig. 2B) and no significant differences in the left putamen ($p_{FDR} = 0.20$).

3.5. Regression analyses

Linear regression did not reveal significant associations of disease duration or ED score in patients with tract integrity measures. Further exploration of structure–function abnormalities in the trajectory $S1_{FACE}$-to-putamen in patients revealed that the change in structural tract integrity by AD showed significant association with average FC ($\beta = 0.60$, $p = 0.013$, $R^2 = 0.36$; Fig. 2B). GM volume in $S1_{FACE}$ was found neither a significant explaining variable of AD nor FC change (adjusted for total intracranial volume; AD: $\beta = 0.10$, $p = 0.74$; FC: $\beta = 0.40$, $p = 0.14$).

3.6. Control analyses

Control analyses evaluating tractography, functional connectivity and grey matter volume in the medial S1 / its projection to the putamen did not observe significant abnormalities in both hemispheres (all $p \geq 0.05$; see table s-4/figure s-3 for details). A control analysis for abnormalities in local functional connectivity (regional homogeneity) between-groups did not reveal significant results ($p_{FWE} > 0.05$). A control analysis for group specificity of the association between AD and FC in the trajectory $S1_{FACE}$-putamen conducted within the group of healthy brass players indicated that this association was specific to the patient group ($R^2 = 0.01$, $\beta = -0.10$, $p = 0.71$).

4. Discussion

We observed bihemispheric AD reduction within projections between $S1_{FACE}$ and the putamen, and converse bihemispheric AD increases within projections between supplementary motor and superior parietal cortex in the patient group. Further, patient's left $S1_{FACE}$ grey matter volume was increased, and left $S1_{FACE}$ FC with the putamen was abnormally reduced; the latter was significantly associated with the AD reduction within the patient group. Increase in MO in patients accompanied the left-hemispheric diffusion abnormalities within the SLF1, and were additionally observed in the supplementary motor area's projection to $M1_{FACE}$.

In the present study, ED patients displayed significantly reduced axial diffusivity in the trajectory connecting the left and right S1 with the respective ipsilateral putamen. At the same time no significant differences in the mode of anisotropy, a measure sensitive to changes in fibre orientation predominance (Douaud et al., 2011), were seen. Axial diffusivity describes linear diffusion of water molecules along aligned fibres in a trajectory. The reduction of such directed diffusion may mirror reduction of equal fibre alignment and has in some animal studies been associated with loss of axonal integrity (Winklewski et al., 2018), though

the inference of a distinct underlying microstructural abnormality from a certain DTI scalar in humans has to date proven difficult. In the left hemisphere, this finding was accompanied by a significant reduction of $S1_{FACE}$-to-putamen functional connectivity, and a significant moderate linear positive relationship between the two abnormalities was seen that was not observed in the patient group. Significant reduction of S1 functional connectivity with the striatum is consistent with a previous observation in (non-task-induced) orofacial dystonia in the resting state

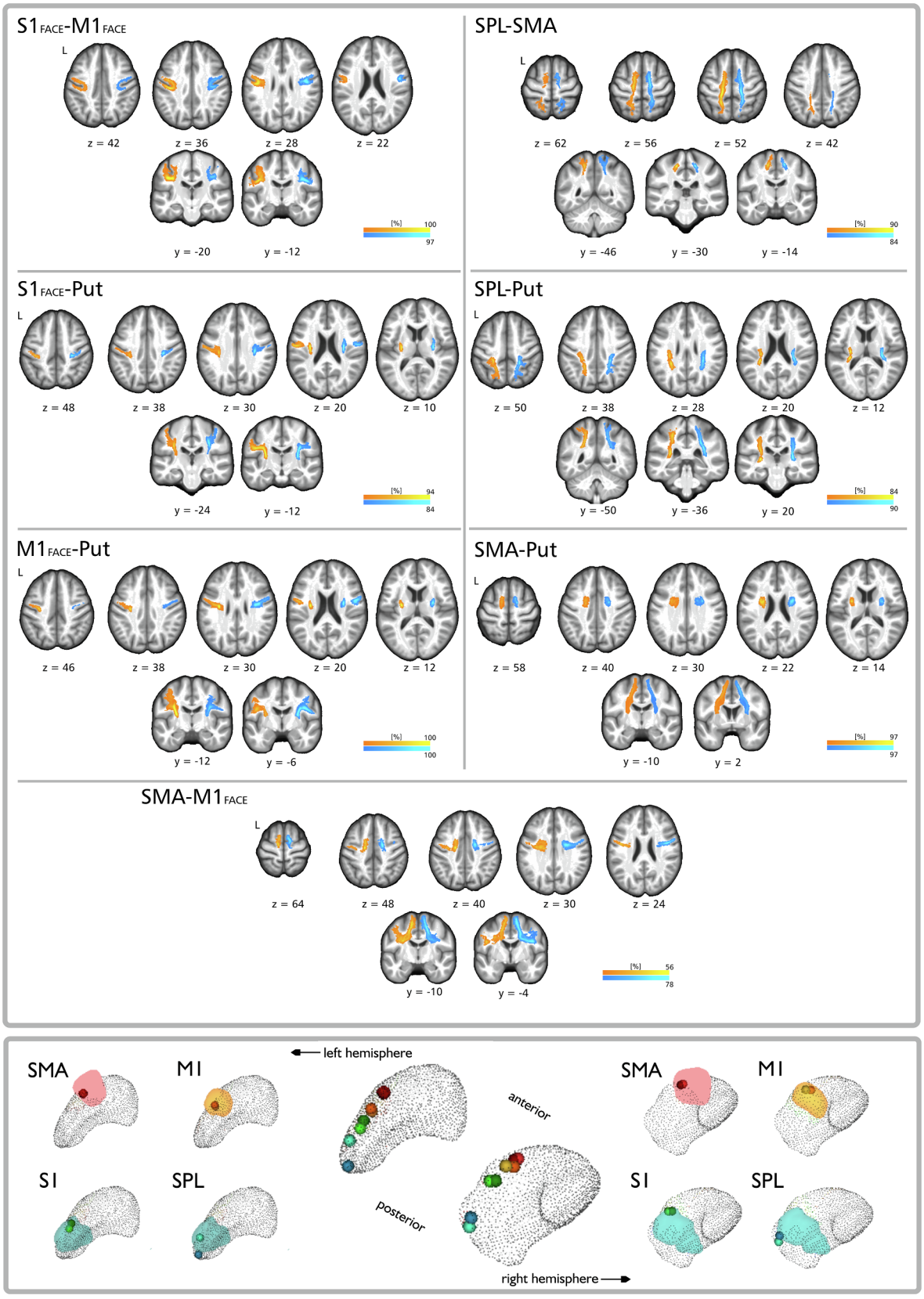

(caption on next page)

Fig. 1. *Upper panel:* Averaged probable trajectories from all participants and for all investigated projections shown in neurological display convention. Probable trajectories involving primary cortices are shown on the left, and trajectories involving higher-order cortices are shown on the right side of the panel. All probable trajectories are displayed at a tract probability threshold of 5%, allowing for visualisation of trajectory-associated variability, with intensities illustrating the percentage of subject overlay at the given threshold (group-wise overlay across probability thresholds is detailed in figure s-2). Warm colors represent tracts in the left, and cold colors represent tracts in the right hemisphere. *Lower panel:* Centroids representing the spatially most likely tract termination in the putamen in each group. Tract terminations followed the known topographic anterior-posterior distribution in the putamen (central column), patients being shown in dark and controls in light colors (centroid coordinates given in table s-5). Tract terminations were further in line with their respective topographic label in the striatal connectivity atlas (Tziortzi et al., 2014) visualized in the lateral columns (centroids projected on the 25% probability maps of striatal connectivity atlas labels: red = rostral motor; orange = caudal motor; blue = parietal). (For interpretation of the references to colour in this figure legend, the reader is referred to the web version of this article.)

(Jochim et al., 2018). Similarly in the task setting, reduced connectivity with S1 was described in writer's cramp patients during dystonic writing using the sensorimotor putamen as seed region (Gallea et al., 2016). The basal ganglia have long been implicated in FD pathophysiology due to their role in the adaptive selection of appropriate motor programs for a desired movement, processing information originating from cortically interconnected areas within functionally (yet not rigidly spatially) segregated cortico-basal-ganglia-cortical loops (Mink, 1996; Wilson, 2014). Particularly the basal ganglia's (somato)sensory circuits have recently gained growing attention for their potential involvement in context-related predictions of sensory outcomes that may modulate action selection during movement(Robbe, 2018; Wilson, 2014). Early work in writer's cramp pointed to a basal ganglia role in the abnormal somatosensory processing in the disease by demonstrating abnormal premovement somatosensory information gating (Murase et al., 2000). Recent positron emission tomography data suggested a hyperfunctionality of the direct basal ganglia output pathway potentially driven by a D1/2 dopamine receptor imbalance encompassing also nonmotor areas of the striatum (Simonyan et al., 2017). In contrast, other previous (mainly electrophysiological) studies favoured disordered inhibitory circuits and homeostatic plasticity within the cortex as basis of the disordered somatosensory processing in FD (Erro et al., 2018; Hallett, 2011). Neuroimaging techniques are limited regarding the differentiation of causative and compensatory changes. It is hence not possible to infer if our new findings of an abnormal link between the sensory cortex and the basal ganglia may be the result of a primary neuronal dysfunction of the primary somatosensory cortex leading to abnormal afferent integration at the striatal level (Conn et al., 2005; Kreitzer and Malenka, 2008; Wall et al., 2013), or the result of a primary (somato)sensory striatal neuronal abnormality facilitating a disinhibition/dysplasticity at the cortical level that subsequently leads to a secondary impairment of its link with the striatum (Quartarone and Hallett, 2013; Simonyan et al., 2017). Brain γ-aminobutyric acid reductions as a potential correlate of impaired inhibitory projections have been observed both in the lentiform nucleus and in the primary sensorimotor cortex of the affected hemisphere in focal hand dystonia patients using magnetic resonance spectroscopy (Levy and Hallett, 2002). While the significant cortico-subcortical tract abnormality reported in this work was confined to sensory trajectories, data in writer's cramp similarly showed a reduction in axial diffusivity in the trajectory connecting the middle frontal gyrus and the putamen (together with fractional anisotropy) (Berndt et al., 2018). This may indicate that other non-sensory cortices undergo comparable changes, though potential FD subtype-associated differences cannot be excluded (Bianchi et al., 2019; Ramdhani et al., 2014). A control analysis of the medial S1 did not reveal similar abnormalities in structural and functional parameters, which might speak against a general underlying character of the above findings within the cortex. Yet, primary somatosensory somatotopy is complex and variable, and establishing reliable somatotopic specificity would require the combination of a functional mapping of such cortices with diffusion imaging, hence warranting confirmation in a accordingly designed event-related fMRI study.

The additionally observed significant increase in left $S1_{FACE}$ GM volume in ED patients fitted a previous observation in the disease using a whole-brain approach (located at a similar level as the ROI used in the present work) and is compatible with findings in other TSFDs (Mantel et al., 2019; Neychev et al., 2011). Yet, there were no significant associations of left $S1_{FACE}$ GM volume with the structure-functional correlates of an impaired link of the area with the putamen. The potential pathophysiologic relation between cortical grey matter volume changes and measures relating to the integrity of related functional or structural projections in FD remains unresolved (Bianchi et al., 2019), complicated by the complex embedding of areas such as S1 within brain connectivity networks (Sepulcre et al., 2012).

Beyond cortico-subcortical abnormalities our findings hinted at altered tract integrity in ED patients within the SLF1, linking the SMA and the SPL. Both cortices have early been identified as important relays for fine motor control during musical performance in the healthy. The SPL is essential for multimodal sensory and spatial processing, and the SMA is a key structure for the execution of internally stored complex movements (e.g. through bihemispheric, top-down and sequential coordination) (Altenmuller, 2003). We observed a significant increase in axial diffusivity in this trajectory in both hemispheres, in the left hemisphere accompanied by a significant mode of anisotropy increase (with a respective right-hemispheric trend that did not survive correction for multiple comparisons). Taken together, this might suggest that (relatively) increased alignment or packing of fibres in this tract could have driven the observed abnormalities through increased diffusion along the fibre's trajectory. The SLF has been proposed to mediate synchronisation of frontoparietal neuronal oscillations implicated in the selective gating of top-down control processes (D'Andrea et al., 2019; Marshall et al., 2015). Our observations might thus hint at a possible facilitation between the two cortices of either compensatory or causative nature. In this regard, interestingly the SMA and SPL have recently both been implicated in premovement sensory facilitation in the presence of reduced/abnormal afferent input (Lhomond et al., 2018). Such dysfunctional afferent input processing both at the central level (also indicated by our above-described finding of sensory cortico-striatal dysconnectivity), and in the periphery (mirrored by abnormal peripheral sensory thresholds) are considered key features in FD (Conte et al., 2019; Stamelou et al., 2012). Moreover, recent work using dynamic causal modelling in laryngeal dystonia (a cranial non-musician TSFD) demonstrated a top-down disruption in sensorimotor network integrity involving the parietal cortex (Battistella and Simonyan, 2019). While the present study focused on a constrained literature-guided sensorimotor model given the expected subtlety of findings in this highly specific disease, parcellating the different components of the SLF to characterize a potential specificity of diffusion abnormalities to certain projections within the fascicle (as far as the technical limitations of diffusion imaging allow) may be of interest for follow-up studies in light of the present findings. Further, while we observed significant diffusion abnormalities in the link between the SMA and M1, a trajectory that is also assumed to mediate top-down motor control, the lack of significant abnormality in other DTI scalars accompanying this change in fibre orientation predominance prevents further interpretation. While unfortunately being beyond the scope of the present study, associating diffusion imaging findings with detailed task fMRI-established mappings of higher-order cortices such as the SMA may be of interest for future work in light of the present results.

In view of the above-described significant abnormalities in the mode of anisotropy within the left SLF1 trajectory and the nature of the measure, it may alternatively be conceivable that a relative reduction in a SLF1-crossing fibre population may have induced or contributed to the observed changes in the predominant fibre orientation and the axial

Table 2
Tract-related white-matter integrity in embouchure-dystonia patients and healthy brass musician controls.

		M1–Put		S1–Put		SMA–Put		SPL–Put
		LH	RH	LH	RH	LH	RH	RH
AD	PAT	0.938 ± 0.007	0.980 ± 0.009	0.974 ± 0.007	0.999 ± 0.005	1.011 ± 0.006	1.022 ± 0.007	1.057 ± 0.007
	CON	0.950 ± 0.006	0.998 ± 0.005	0.998 ± 0.008	1.022 ± 0.008	1.002 ± 0.010	1.016 ± 0.011	1.048 ± 0.010
	t	1.755	2.189	2.635	2.680	−0.426	0.100	−0.967
	P_{unc}	0.091	0.038	0.014	0.011	0.683	0.922	0.343
	P_{FDR}	0.181	0.106	**0.049**	**0.049**	0.922	0.922	0.601
MO	PAT	0.396 ± 0.031	0.438 ± 0.022	0.307 ± 0.030	0.46 ± 0.028	0.548 ± 0.018	0.585 ± 0.017	0.494 ± 0.025
	CON	0.448 ± 0.023	0.479 ± 0.018	0.38 ± 0.033	0.534 ± 0.026	0.472 ± 0.040	0.546 ± 0.030	0.464 ± 0.032
	t	1.700	1.055	1.585	1.706	−1.671	−0.986	−0.926
	P_{unc}	0.096	0.297	0.126	0.100	0.090	0.334	0.372
	P_{FDR}	0.200	0.461	0.22	0.200	0.200	0.467	0.473

	SPL–Put	M1–S1		SMA–M1		SMA–SPL	
	RH	LH	RH	LH	RH	LH	RH
AD	1.086 ± 0.01	0.944 ± 0.005	0.943 ± 0.007	0.985 ± 0.012	1.005 ± 0.010	1.048 ± 0.012	1.05 ± 0.013
	1.082 ± 0.009	0.947 ± 0.004	0.953 ± 0.007	0.979 ± 0.008	0.998 ± 0.013	0.997 ± 0.014	0.999 ± 0.012
	−0.295	0.447	1.821	0.227	−0.176	−2.647	−2.758
	0.770	0.656	0.078	0.822	0.865	0.014	0.012
	0.922	0.922	0.181	0.922	0.922	**0.049**	**0.049**
MO	0.524 ± 0.028	0.275 ± 0.023	0.252 ± 0.032	0.427 ± 0.017	0.416 ± 0.026	0.372 ± 0.035	0.351 ± 0.036
	0.528 ± 0.021	0.207 ± 0.020	0.217 ± 0.024	0.316 ± 0.031	0.434 ± 0.024	0.163 ± 0.042	0.243 ± 0.046
	0.122	−2.158	−0.490	−3.697	−2.181	−3.190	0.1109
	0.905	0.040	0.628	0.009	0.038	0.003	0.914
	0.914	0.140	0.732	**0.018**	0.914	**0.013**	0.914

Average axial diffusivity AD (given in $10^{-3}mm^2s^{-1}$) and mode of anisotropy MO within the seven investigated tracts in the left and right hemisphere in patients (PAT) and musician controls (CON). Results are displayed as mean ± standard error of the mean. P-value estimates of the two-tailed between-group comparisons were based on 100,000 permutations. All p-values were FDR-corrected for 14 analysed tracts. Results for other DTI scalars FA, RD are given in the supplement.

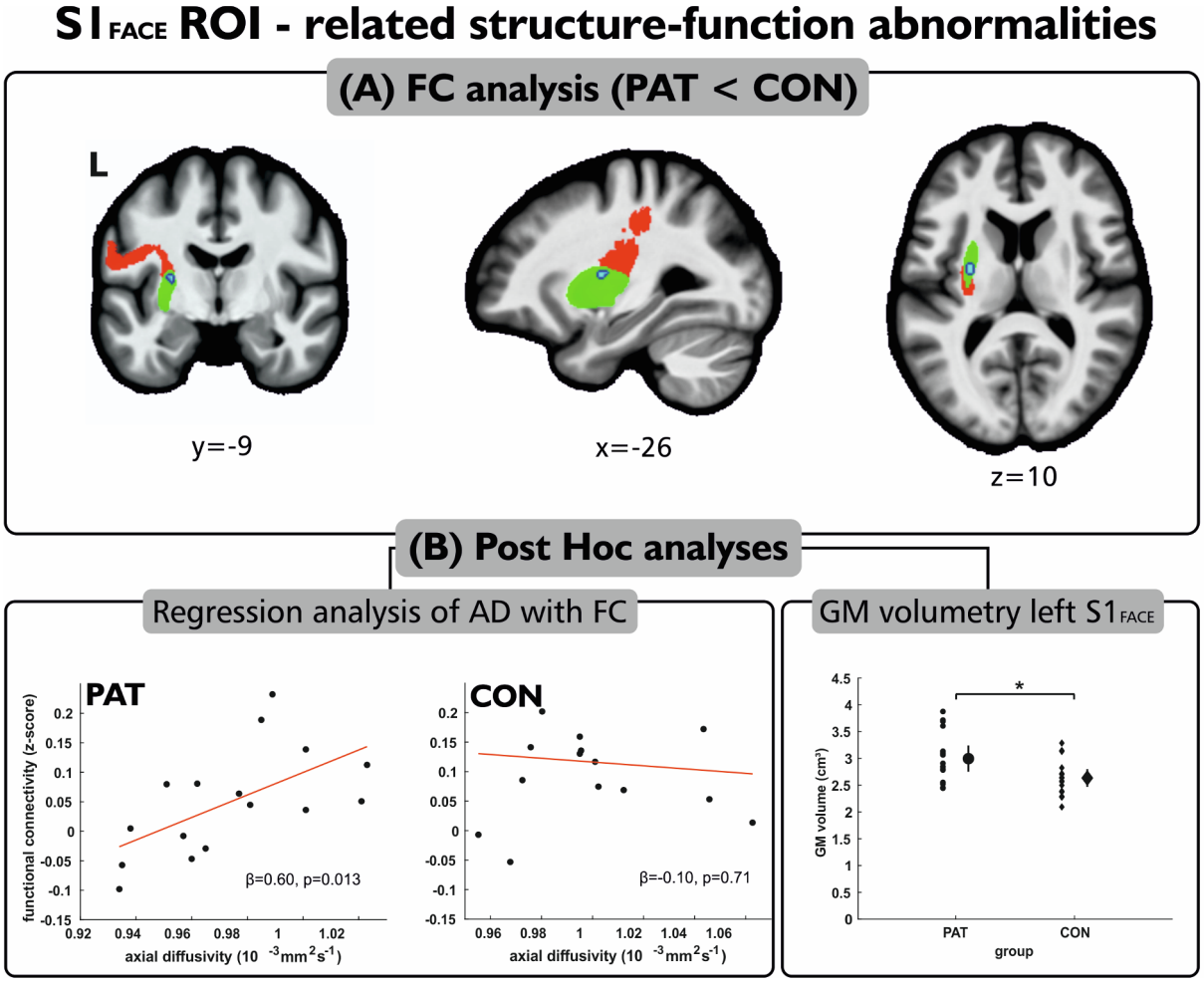

Fig. 2. (A) Results of the FC analysis showing reduced left $S1_{FACE}$ FC (in blue) with the putamen (highlighted in green). The area of altered FC within the putamen was spatially located beneath the terminations of the cortico-subcortical tract from S1 to the putamen (visualized through the overlaid averaged tract from Fig. 1, shown in red). (B) Results of post hoc analyses. The left panels depict the results of the regression analysis for both groups showing moderate significant positive association of the average axial diffusivity in the trajectory between $S1_{FACE}$ and the putamen with the average FC with the putamen (extracted from a 10 mm sphere around the significant cluster's peak coordinate). The right panel illustrated the result of the post-hoc GM volume analysis in the S1 ROI in patients (filled circles) and controls (filled diamonds). Error bars depict the double standard error of mean. (For interpretation of the references to colour in this figure legend, the reader is referred to the web version of this article.)

diffusivity. Yet in this area, the trunk or foot somatotopic sensorimotor representations would be origin or destination of the main crossing trajectories. While a spread of task-specific dystonic symptoms to the hand (i.e. writer's cramp) in ED along the disease course has been described in some patients and discussed within the concept of an endophenotype potentially mirrored by functional MRI abnormalities in the respective primary somatosensory somatotopic representation, a dystonic involvement of the trunk or foot is unlikely in consideration of previous observations in ED (Frucht, 2009; Haslinger et al., 2010, 2017; Mantel et al., 2019, 2016), and we did not observe abnormalities in a control analyses of the projection from the medial S1 to the putamen. Functionally, we did not observe abnormal SMA or SPL resting FC. The reason for this beyond general methodological constraints of seed-based resting-state FC analyses remains unresolved. Studies focusing on differential characterization of higher-order parieto-premotor connectivity are unfortunately sparse in TSFD. One study in writer's cramp observed reduced resting connectivity in the SPL seeding from the dorsal premotor cortex, but did not investigate the SMA (Delnooz et al., 2012).

Our description of abnormal white matter integrity in sensory trajectories in patients supports the key role of the sensory system in ED, although the lack of abnormal fractional anisotropy as a more common measure of tract integrity is a limitation of this work. The reasons remain ultimately unclear, yet method-associated aspects owed to the focus on tract-averaged measures cannot be excluded. For instance, tract-averaged measures may make focal abnormalities potentially less influential compared to voxel-based or tract segment-focused statistics given the long course of the investigated tracts.

The overall majority of previous diffusion imaging studies comparing white matter integrity in TSFD against healthy controls did not conduct evaluations based on whole-tract measures but focused on the voxel level, and findings at the cortical level were rarely reported (Neychev et al., 2011): A recent study found an isolated focal reduction of fractional anisotropy beneath the precuneus comparing a mixed TSFD collective against healthy controls using tract-based spatial statistics (Bianchi et al., 2019). One study in writer's cramp investigating voxel-wise differences within the normalized across-group primary sensorimotor corticospinal tract volume described abnormal subcortical (internal capsule and below) fractional anisotropy (Delmaire et al., 2009). Other diffusion imaging investigations in TSFD mainly relied on selected ROI analyses without reconstruction of distinct trajectories and reported mostly abnormalities below the cortical level: in the internal capsule, cerebral and middle cerebellar peduncle in laryngeal dystonia, and the internal capsule in focal hand dystonia (Neychev et al., 2011). Overall, this sparsity of diffusion imaging studies in TSFD (especially

with regard to tract-level analyses) as well as the technical heterogeneity of previous investigations underlines the necessity of further work to characterize the abnormal structural connectome in the disease. In this regard, our observation of abnormalities in the mode of anisotropy may be of particular interest, as to our knowledge, measures sensitive to changes in fibre orientation predominance have not yet been employed in previous diffusion imaging studies in FD.

5. Conclusion

The first-time observation of correlates of reduced structural (-functional) integrity in the primary somatosensory cortico-putaminal trajectory might point to an impairment of afferent sensory input to the putamen in the context of abnormal somatosensory processing in ED. Abnormalities within the higher-order cortico-cortical sensorimotor projections of the superior longitudinal fascicle might hint at cortical sensorimotor facilitation processes of either dysfunctional or compensatory nature.

Ethics approval

The study has been approved by the local ethics review board and written informed consent was obtained from all subjects.

Funding

This study was supported by the Deutsche Forschungsgemeinschaft (DFG HA3370/5-1) Bonn, Germany and the Kommission für Klinische Forschung, Technical University of Munich School of Medicine (KKF H-05).

CRediT authorship contribution statement

Tobias Mantel: Investigation, Formal analysis, Methodology, Visualization, Writing - original draft, Writing - review & editing. **Eckart Altenmüller:** Investigation, Resources, Writing - review & editing. **Yong Li:** Investigation, Validation, Data curation. **Tobias Meindl:** Writing - review & editing. **Angela Jochim:** Writing - review & editing. **André Lee:** Validation, Writing - review & editing. **Claus Zimmer:** Resources, Writing - review & editing. **Bernhard Haslinger:** Conceptualization, Funding acquisition, Resources, Project administration, Supervision, Writing - review & editing.

Acknowledgments

We cordially thank all musicians for their participation in the study.

Appendix A. Supplementary data

Supplementary data to this article can be found online at https://doi.org/10.1016/j.nicl.2020.102410.

References

Altenmuller, E., 2003. Focal dystonia: advances in brain imaging and understanding of fine motor control in musicians. Hand. Clin. 19 (523–538), xi.
Battistella, G., Simonyan, K., 2019. Top-down alteration of functional connectivity within the sensorimotor network in focal dystonia. Neurology 92, e1843–e1851.
Berndt, M., Li, Y., Gora-Stahlberg, G., Jochim, A., Haslinger, B., 2018. Impaired white matter integrity between premotor cortex and basal ganglia in writer's cramp. Brain Behav. 8, e01111.
Bianchi, S., Fuertinger, S., Huddleston, H., Frucht, S.J., Simonyan, K., 2019. Functional and structural neural bases of task specificity in isolated focal dystonia. Mov. Disord. 34, 555–563.
Bozkurt, B., Yagmurlu, K., Middlebrooks, E.H., Cayci, Z., Cevik, O.M., Karadag, A., Moen, S., Tanriover, N., Grande, A.W., 2017. Fiber connections of the supplementary motor area revisited: methodology of fiber dissection, DTI, and three dimensional documentation. J. Vis. Exp.
Conn, P.J., Battaglia, G., Marino, M.J., Nicoletti, F., 2005. Metabotropic glutamate receptors in the basal ganglia motor circuit. Nat. Rev. Neurosci. 6, 787–798.
Conte, A., Defazio, G., Hallett, M., Fabbrini, G., Berardelli, A., 2019. The role of sensory information in the pathophysiology of focal dystonias. Nat. Rev. Neurol. 15, 224–233.
D'Andrea, A., Chella, F., Marshall, T.R., Pizzella, V., Romani, G.L., Jensen, O., Marzetti, L., 2019. Alpha and alpha-beta phase synchronization mediate the recruitment of the visuospatial attention network through the Superior Longitudinal Fasciculus. Neuroimage 188, 722–732.
Delmaire, C., Vidailhet, M., Wassermann, D., Descoteaux, M., Valabregue, R., Bourdain, F., Lenglet, C., Sangla, S., Terrier, A., Deriche, R., Lehericy, S., 2009. Diffusion abnormalities in the primary sensorimotor pathways in writer's cramp. Arch. Neurol. 66, 502–508.
Delnooz, C.C., Helmich, R.C., Toni, I., van de Warrenburg, B.P., 2012. Reduced parietal connectivity with a premotor writing area in writer's cramp. Mov. Disord. 27, 1425–1431.
Douaud, G., Jbabdi, S., Behrens, T.E., Menke, R.A., Gass, A., Monsch, A.U., Rao, A., Whitcher, B., Kindlmann, G., Matthews, P.M., Smith, S., 2011. DTI measures in crossing-fibre areas: increased diffusion anisotropy reveals early white matter alteration in MCI and mild Alzheimer's disease. Neuroimage 55, 880–890.
Erro, R., Rocchi, L., Antelmi, E., Liguori, R., Tinazzi, M., Berardelli, A., Rothwell, J., Bhatia, K.P., 2018. High frequency somatosensory stimulation in dystonia: Evidence fordefective inhibitory plasticity. Mov. Disord. 33, 1902–1909.
Fan, L., Li, H., Zhuo, J., Zhang, Y., Wang, J., Chen, L., Yang, Z., Chu, C., Xie, S., Laird, A.R., Fox, P.T., Eickhoff, S.B., Yu, C., Jiang, T., 2016. The human Brainnetome atlas: a new brain atlas based on connectional architecture. Cereb. Cortex 26, 3508–3526.
Frucht, S.J., 2009. Embouchure dystonia–Portrait of a task-specific cranial dystonia. Mov. Disord. 24, 1752–1762.
Fujita, K., Eidelberg, D., 2017. Imbalance of the direct and indirect pathways in focal dystonia: a balanced view. Brain 140, 3075–3077.
Gallea, C., Horovitz, S.G., Najee-Ullah, M., Hallett, M., 2016. Impairment of a parieto-premotor network specialized for handwriting in writer's cramp. Hum. Brain Mapp. 37, 4363–4375.
Granert, O., Peller, M., Jabusch, H.C., Altenmuller, E., Siebner, H.R., 2011. Sensorimotor skills and focal dystonia are linked to putaminal grey-matter volume in pianists. J. Neurol. Neurosurg. Psychiatry 82, 1225–1231.
Hallett, M., 2011. Neurophysiology of dystonia: the role of inhibition. Neurobiol. Dis. 42, 177–184.
Haslinger, B., Altenmuller, E., Castrop, F., Zimmer, C., Dresel, C., 2010. Sensorimotor overactivity as a pathophysiologic trait of embouchure dystonia. Neurology 74, 1790–1797.
Haslinger, B., Noe, J., Altenmuller, E., Riedl, V., Zimmer, C., Mantel, T., Dresel, C., 2017. Changes in resting-state connectivity in musicians with embouchure dystonia. Mov. Disord. 32, 450–458.
Irfanoglu, M.O., Walker, L., Sarlls, J., Marenco, S., Pierpaoli, C., 2012. Effects of image distortions originating from susceptibility variations and concomitant fields on diffusion MRI tractography results. Neuroimage 61, 275–288.
Jenkinson, M., Bannister, P., Brady, M., Smith, S., 2002. Improved optimization for the robust and accurate linear registration and motion correction of brain images. Neuroimage 17, 825–841.
Jeurissen, B., Descoteaux, M., Mori, S., Leemans, A., 2019. Diffusion MRI fiber tractography of the brain. NMR Biomed. 32, e3785.
Jiang, L., Zuo, X.N., 2016. Regional homogeneity: a multimodal, multiscale neuroimaging marker of the human connectome. Neuroscientist 22, 486–505.
Jochim, A., Li, Y., Gora-Stahlberg, G., Mantel, T., Berndt, M., Castrop, F., Dresel, C., Haslinger, B., 2018. Altered functional connectivity in blepharospasm/orofacial dystonia. Brain Behav. 8, e00894.
Kamali, A., Flanders, A.E., Brody, J., Hunter, J.V., Hasan, K.M., 2014. Tracing superior longitudinal fasciculus connectivity in the human brain using high resolution diffusion tensor tractography. Brain Struct. Funct. 219, 269–281.
Kita, K., Rokicki, J., Furuya, S., Sakamoto, T., Hanakawa, T., 2018. Resting-state basal ganglia network codes a motor musical skill and its disruption from dystonia. Mov. Disord. 33, 1472–1480.
Kreitzer, A.C., Malenka, R.C., 2008. Striatal plasticity and basal ganglia circuit function. Neuron 60, 543–554.
Leemans, A., Jones, D.K., 2009. The B-matrix must be rotated when correcting for subject motion in DTI data. Magn. Reson. Med. 61, 1336–1349.
Lehericy, S., Ducros, M., Van de Moortele, P.F., Francois, C., Thivard, L., Poupon, C., Swindale, N., Ugurbil, K., Kim, D.S., 2004. Diffusion tensor fiber tracking shows distinct corticostriatal circuits in humans. Ann. Neurol. 55, 522–529.
Levy, L.M., Hallett, M., 2002. Impaired brain GABA in focal dystonia. Ann. Neurol. 51, 93–101.
Lhomond, O., Teasdale, N., Simoneau, M., Mouchnino, L., 2018. Supplementary motor area and superior parietal lobule restore sensory facilitation prior to stepping when a decrease of afferent inputs occurs. Front. Neurol. 9, 1132.
Lim, V.K., Bradshaw, J.L., Nicholls, M.E., Altenmuller, E., 2003. Perceptual differences in sequential stimuli across patients with musician's and writer's cramp. Mov. Disord. 18, 1286–1293.
Makris, N., Kennedy, D.N., McInerney, S., Sorensen, A.G., Wang, R., Caviness Jr., V.S., Pandya, D.N., 2005. Segmentation of subcomponents within the superior longitudinal fascicle in humans: a quantitative, in vivo, DT-MRI study. Cereb. Cortex 15, 854–869.
Mantel, T., Altenmuller, E., Li, Y., Meindl, T., Jochim, A., Lee, A., Zimmer, C., Dresel, C., Haslinger, B., 2019. Abnormalities in grey matter structure in embouchure dystonia. Parkinsonism Relat. Disord. 65, 111–116.
Mantel, T., Dresel, C., Altenmuller, E., Zimmer, C., Noe, J., Haslinger, B., 2016. Activity and topographic changes in the somatosensory system in embouchure dystonia. Mov. Disord. 31, 1640–1648.

Marshall, T.R., Bergmann, T.O., Jensen, O., 2015. Frontoparietal structural connectivity mediates the top-down control of neuronal synchronization associated with selective attention. PLoS Biol. 13, e1002272.
Mink, J.W., 1996. The basal ganglia: focused selection and inhibition of competing motor programs. Prog. Neurobiol. 50, 381–425.
Murase, N., Kaji, R., Shimazu, H., Katayama-Hirota, M., Ikeda, A., Kohara, N., Kimura, J., Shibasaki, H., Rothwell, J.C., 2000. Abnormal premovement gating of somatosensory input in writer's cramp. Brain 123 (Pt 9), 1813–1829.
Neychev, V.K., Gross, R.E., Lehericy, S., Hess, E.J., Jinnah, H.A., 2011. The functional neuroanatomy of dystonia. Neurobiol Dis 42, 185–201.
Oldfield, R.C., 1971. The assessment and analysis of handedness: the Edinburgh inventory. Neuropsychologia 9, 97–113.
Quartarone, A., Hallett, M., 2013. Emerging concepts in the physiological basis of dystonia. Mov. Disord. 28, 958–967.
Ramdhani, R.A., Kumar, V., Velickovic, M., Frucht, S.J., Tagliati, M., Simonyan, K., 2014. What's special about task in dystonia? A voxel-based morphometry and diffusion weighted imaging study. Mov. Disord. 29, 1141–1150.
Robbe, D., 2018. To move or to sense? Incorporating somatosensory representation into striatal functions. Curr. Opin. Neurobiol. 52, 123–130.
Rosenkranz, K., Williamon, A., Butler, K., Cordivari, C., Lees, A.J., Rothwell, J.C., 2005. Pathophysiological differences between musician's dystonia and writer's cramp. Brain 128, 918–931.
Schulz, R., Koch, P., Zimerman, M., Wessel, M., Bonstrup, M., Thomalla, G., Cheng, B., Gerloff, C., Hummel, F.C., 2015. Parietofrontal motor pathways and their association with motor function after stroke. Brain 138, 1949–1960.
Sepulcre, J., Sabuncu, M.R., Yeo, T.B., Liu, H., Johnson, K.A., 2012. Stepwise connectivity of the modal cortex reveals the multimodal organization of the human brain. J. Neurosci. 32, 10649–10661.
Simonyan, K., Cho, H., Hamzehei Sichani, A., Rubien-Thomas, E., Hallett, M., 2017. The direct basal ganglia pathway is hyperfunctional in focal dystonia. Brain 140, 3179–3190.
Stamelou, M., Edwards, M.J., Hallett, M., Bhatia, K.P., 2012. The non-motor syndrome of primary dystonia: clinical and pathophysiological implications. Brain 135, 1668–1681.
Tziortzi, A.C., Haber, S.N., Searle, G.E., Tsoumpas, C., Long, C.J., Shotbolt, P., Douaud, G., Jbabdi, S., Behrens, T.E., Rabiner, E.A., Jenkinson, M., Gunn, R.N., 2014. Connectivity-based functional analysis of dopamine release in the striatum using diffusion-weighted MRI and positron emission tomography. Cereb. Cortex 24, 1165–1177.
Uehara, K., Furuya, S., Numazawa, H., Kita, K., Sakamoto, T., Hanakawa, T., 2019. Distinct roles of brain activity and somatotopic representation in pathophysiology of focal dystonia. Hum. Brain Mapp. 40, 1738–1749.
Wall, N.R., De La Parra, M., Callaway, E.M., Kreitzer, A.C., 2013. Differential innervation of direct- and indirect-pathway striatal projection neurons. Neuron 79, 347–360.
Wilson, C.J., 2014. The sensory striatum. Neuron 83, 999–1001.
Winkler, A.M., Ridgway, G.R., Webster, M.A., Smith, S.M., Nichols, T.E., 2014. Permutation inference for the general linear model. Neuroimage 92, 381–397.
Winkler, A.M., Webster, M.A., Brooks, J.C., Tracey, I., Smith, S.M., Nichols, T.E., 2016. Non-parametric combination and related permutation tests for neuroimaging. Hum. Brain Mapp. 37, 1486–1511.
Winklewski, P.J., Sabisz, A., Naumczyk, P., Jodzio, K., Szurowska, E., Szarmach, A., 2018. Understanding the physiopathology behind axial and radial diffusivity changes-what do we know? Front. Neurol. 9, 92.